Dalton Transactions

ROYAL SOCIETY OF CHEMISTRY

PAPER

Cite this: *Dalton Trans.*, 2022, **51**, 13368

Bicyclopeptides: a new class of ligands for Cu(II) ions†

Aleksandra Marciniak, [a] Lorenzo Pacini, [b,c] Anna Maria Papini [b,c] and Justyna Brasuń *[a]

Received 13th May 2022,
Accepted 2nd August 2022

DOI: 10.1039/d2dt01497a

rsc.li/dalton

There is growing interest in bicyclic peptides among scientists. This group of compounds has more advantageous properties than monocyclic ligands and their application in medicine and biological sciences is possible. It is known that sometimes the presence of metal ions is crucial for the activity of peptides in biological systems, like in the case of oxytocin or vasopressin. Therefore, in this study, we performed a series of experiments with the new bicyclic peptide c(PKKHP-c(CFWKTC)-PKKH) (**BCL**) that was designed and synthesized by a fully automated induction-assisted solid phase synthesizer. We analyzed the coordination abilities of **BCL** relative to copper(II) ions. The new bicyclic peptide contains two histidine moieties, separated by proline residues, with two distinct sites for metal ion coordination. The obtained results showed that in all analyzed systems both mono- and dinuclear complexes are formed.

1. Introduction

Bicyclic peptides are a very promising class of compounds. Compared to monocyclic molecules, they have many advantages, such as increased stability and membrane permeability and higher selectivity possibly because of lower flexibility than linear or monocyclic peptides.[1] Moreover, each ring can fulfill different functions, for example, the first ring can be responsible for binding to the target and the second one can favor cell penetration. Therefore, these molecules are also termed chimeras.[2] So far, many bicyclic peptides have also been discovered as natural products in plants, fungi, and animals, displaying different biological properties, such as moroidin from *Celosia argentea*, phalloidin from *Amanita phalloides*, and theonellamides A–G from a marine sponge.[3–5] Some of them are already used as drugs or are under different clinical phases. Among them, we can mention romidepsin isolated from *Chromobacterium violaceum* bacteria and used in peripheral T-cell lymphomas, or bouvardin which is used as an anticancer agent.[2,6,7] Some bicyclic peptides can be used as cell surface receptor agonists and antagonists in targeted therapy, and as PET tracers or imaging agents, such as somatostatin analogs.[2,8–10] Therefore, the approach based on the design of new synthetic bicyclic peptides with particular binding abilities toward bio-metal ions is challenging for further research and development. In particular, the interaction of complexes of metal ions with peptides and proteins is the basis of their storage, transport, biological function, and toxicity. Divalent metal ions such as copper and zinc have an important role in regulating biological processes related to the endocrine system.[11] Metal ions bind to DNA and transcription factors, thereby respectively facilitating and inhibiting the transcription process during peptide hormone synthesis.[12] They can bind to hormones after translation, affecting the stability of the resulting compounds. Furthermore, peptide hormones are subjected to post-translational modifications involving metal ion-dependent peptidases.[13–15] Metal ions affect peptide hormone conformation after secretion. Accordingly, they inhibit or stimulate their biological activity. They also play an important role in binding to specific receptors, which greatly facilitates hormone–receptor interactions.[16,17]

Previous studies have shown that copper ions binding to vasopressin enhance and modify the contractile activity of this hormone. It stabilizes the π–π interactions between phenylalanine and tyrosine side chains, which are actively involved in the interaction with the receptor.[18] Similar interactions were observed between metal ions and oxytocin.[17] Moreover, the coordination of zinc(II) ions with oxytocin has affected hormone conformation significantly, facilitating its binding to the receptor.[19] This experiment was also confirmed with other divalent metal ions.[20,21] By studying these interactions, it is possible to design new drugs and effective diagnostic targets.

[a]*Department of Inorganic Chemistry, Wroclaw Medical University, Borowska 211A, 50-556 Wroclaw, Poland. E-mail: justyna.brasun@umw.edu.pl; Fax: +48 71 784 03 36; Tel: +48 71 784 03 30*

[b]*Interdepartmental Research Unit of Peptide and Protein Chemistry and Biology, Department of Chemistry "Ugo Schiff", University of Florence, Via Della Lastruccia 13, 50019 Sesto Fiorentino, Italy. E-mail: l.pacini@unifi.it*

[c]*MoD&LS Laboratory, University of Florence, Centre of Competences RISE, Via Madonna del Piano 6, 50019 Sesto Fiorentino, Italy*

† Electronic supplementary information (ESI) available. See DOI: https://doi.org/10.1039/d2dt01497a

This journal is © The Royal Society of Chemistry 2022

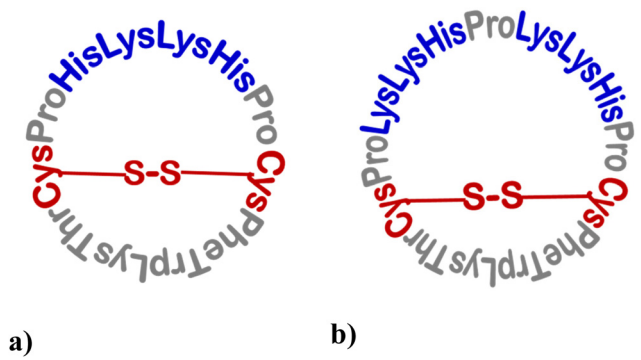

Fig. 1 The schematic structure of the ligands **BCS**, c(-c(CFWKTC)-PHKKHP) (a) and **BCL**, c(PKKHP-c(CFWKTC)-PKKH) (b). The sequence of the metal binding domain is shown in blue.

The first studies on coordination properties that were performed with the bicyclic peptide **BCS**, **c(-c(CFWKTC)-PHKKHP)** (Fig. 1a), have shown that binding of Cu(II) ions takes place by complexing directly the peptide backbone and the imidazolyl side chain of histidines unusually in a more stable way than His-complexes formed by different peptide sequences.[22–26] Therefore, in the present work, we investigated the metal binding properties of the newly designed bicyclic ligand **BCL** characterized by the sequence **c(PKKHP-c(CFWKTC)-PKKH)** (Fig. 1b). Due to the presence of proline residues, two separate binding domains are present in the peptide molecule. The studies were performed for three systems with different ligand to metal ion molar ratios of 2 : 1 (**A** system), 1 : 1 (**B** system), and 1 : 2 (**C** system). The binding properties of **BCL** were characterized by UV-Vis spectroscopy, magnetic circular dichroism spectroscopy, and potentiometric titration.

2. Experimental section

2.1. Materials

The bicyclic peptide c(-c(CFWKTC)-PHKKHP) (**BCS**, Fig. 1a) was purchased by the STI company (Poland) and prepared as previously described.[27] The bicyclic peptide c(PKKHP-c(CFWKTC)-PKKH) (**BCL**, Fig. 1b), designed for the present study, was synthesized and purified using the procedure described below (Section 2.2. Peptide synthesis).

2.2. Peptide synthesis

The bicyclic peptide **BCL** was prepared by fully automated induction-assisted solid phase peptide synthesis (Gyros Protein Technologies, PurePep®Chorus®, Gyros Protein Technologies, Tucson AZ, USA) following the three-dimensional orthogonal protection strategy Fmoc/*t*Bu/Allyl.[28,29] The synthesis started by anchoring the imidazole ring of the histidine residue in the building block Fmoc-L-His-OAll to the trityl chloride-resin under mechanical stirring.[30] The quantity of the amino acid was specifically chosen in order to obtain a final loading of around 0.2–0.4 mmol g^{-1}.

The Fmoc/*t*Bu/Allyl induction assisted SPPS protocol at a 50 μmol scale consisted of (1) swelling in DMF (3 mL) for 30 min, r.t.; (2) double deprotection for 5 min, r.t. (20% piperidine in DMF, 3 mL); (3) washing with DMF (3 × 2 mL); (4) coupling: Fmoc-L-aa-OH, HATU, and DiPEA (5 : 5 : 10), 30 min, r.t.; and (5) washing with DMF (2 mL). Peptide elongation was performed by repeating this general protocol for each amino acid adequately and orthogonally protected as follows: Fmoc-L-Cys(Trt)-OH, Fmoc-L-Phe-OH, Fmoc-L-Trp(Boc)-OH, Fmoc-L-Lys(Boc)-OH, Fmoc-L-Thr(*t*Bu)-OH, Fmoc-L-Pro-OH, and Fmoc-L-His(Trt)-OH.

Both the deprotection and coupling reactions were performed in a glass vessel under mechanical mixing and nitrogen bubbling. After the last cycle, the allyl group on the anchored His residue was removed with $Pd(PPh_3)_4$ (3 eq.) in $CHCl_3$/AcOH/NMM (37 : 2 : 1) under Ar for 3 h at r.t. Then the resin was washed with DiPEA/DMF (0.5 : 99.5) and sodium diethyldithiocarbamate in DMF (0.5 : 99.5).

After Fmoc removal, the cyclization of the linear peptide anchored to the resin (300 mg) was performed by treatment with DiPEA (4 eq.) and TBTU (2 eq.) in DMF (3 mL) until the Kaiser test is negative. After washing with DMF and DCM (3 × 3 mL g^{-1} resin), the resin was dried under vacuum. The cleavage of the peptide from the resin, with concomitant deprotection of acid labile amino-acid side-chains, was achieved by treatment of the peptide-resin with a cocktail of TFA/TIS/H_2O (10 mL, 95 : 2.5 : 2.5). The cleavage was carried out for 2.5 h at r.t. under magnetic stirring. The resin was filtered and rinsed with fresh TFA. The cleavage mixture was precipitated by the addition of ice-cold Et_2O (20 mL). The precipitated crude cyclopeptide precursor was washed with ice-cold Et_2O (4 × 20 mL) and dried under vacuum.

The crude head-to-tail cyclopeptide with free cysteine residues was solubilized in a mixture of water and CH_3CN (1 : 1) and then stirred for about 15 min to perform the reaction of intramolecular disulfide bond formation. After complete dissolution, additional water was added to the reaction mixture to obtain a final concentration of 5.3 mM. Initially, the measured pH, being 2.5, was adjusted to 9.5 by adding NH_4OH 7.5%. H_2O_2 (0.8 eq.) was added and the mixture was mechanically stirred for 2 h at 350 rpm at room temperature. Finally, the reaction was quenched by adding TFA and adjusting the pH to 2.5. Then the reaction mixture was lyophilized without further evaporation.

The crude bicyclic peptide **BCL** (HPLC purity >60%) was purified by reverse-phase flash chromatography monitored with a UV detector (Teledyne ISCO Combi*Flash* NextGen 300+, Lincoln NE, USA) using a column SNAP Ultra C18 (30 g), Column Volume (CV) 45 mL; flow: 25 mL min^{-1}; eluents: 0.1% TFA in H_2O (A) and 0.1% TFA in CH_3CN (B); gradient: 3 CV A, 10 CV from 0% to 50% B, 3 CV B. After lyophilization, the desired bicyclic peptide **BCL** was obtained as a white powder (HPLC purity 93%). The characterization of the peptide **BCL** was performed by RP-UHPLC-MS using a Thermo Scientific Ultimate 3000 equipped with a diode array detector and a Thermo Scientific-MSQ PLUS, using a C18 Waters Acquity

CSH™ (130 Å, 1.7 μm, 2.1 × 100 mm); temperature 318.15 °K; flow rate: 0.5 mL min^{-1}; eluents: 0.1% TFA in H_2O (A) and 0.1% TFA in CH_3CN (B), λ 215 nm. **BCL** peptide: c(PKKHP-c(CFWKTC)-PKKH); $[M + H]^+$ calcd 1844.95; $[M + H]^+$ found 1844.83. HPLC purity: 93%. Further purification of the lyophilized peptide was performed using a semi-preparative RP-HPLC Waters 600 instrument (Milford, MA, USA), equipped with a Waters 2487 UV detector model using a C18 BioSepax™ column (200 Å, 5 μm 10 × 150 mm); temperature 298.15 °K; flow rate: 4.0 mL min^{-1}; eluents: 0.1% TFA in H_2O (A) and 0.1% TFA in CH_3CN (B), gradient: 25–60% (v/v) B in A in 40 min; λ 215 nm. The eluted fractions were analysed by RP-UHPLC-MS using a Thermo Scientific Ultimate 3000 equipped with a diode array detector and a Thermo Scientific-MSQ PLUS, using a C18 Waters Acquity CSH™ (130 Å, 1.7 μm, 2.1 × 100 mm); temperature 318.15 °K; flow rate: 0.5 mL min^{-1}; eluents: 0.1% TFA in H_2O (A) and 0.1% TFA in CH_3CN (B), λ 215 nm; gradient: 5% to 95% B in A in 5 min. The homogeneous fractions corresponding to Rt: 3.27 min were pooled and lyophilized. **BCL** peptide: c(PKKHP-c(CFWKTC)-PKKH) (11.5 mg, yield 7.7%): $[M + H]^+$ calcd 1844.95; $[M + H]^+$ found 1844.83. UHPLC purity: 98.55% (Fig. S1 presented in the ESI†)

2.3. Potentiometric measurements

Potentiometric measurements were carried out by using a Metrohm pH-meter system using a Methrohm semi-micro combination electrode at 25 °C calibrated at a hydrogen ion concentration using HCl.[31] The ligand concentration was 6×10^{-4} mol L^{-1} and the pH-metric titrations were performed in a 0.3 mol L^{-1} KCl solution using a sample volume of 1.5 mL. Potassium hydroxide (KOH) was added using a 2 mL micrometer syringe. The KOH concentration was 0.1 mol L^{-1}. Measurements were carried out in the 2.5–11.5 pH range. The stability constants and stoichiometry of the complexes were calculated using the titration curves and the HYPERQUAD and SUPERQUAD software.[32,33]

2.4. Spectroscopic measurements

Visible spectra were recorded at 25 °C using a Varian Cary 50 Bio spectrophotometer (Varian Inc., USA) in the 300–800 nm range. Magnetic circular dichroism (MCD) spectra were recorded using a Jasco J-1500 spectrometer (Jasco, Japan) in the 230–800 nm range at 25 °C for all investigated systems. The spectra were collected at a scan rate of 100 nm min^{-1} with a response time of 1 s. A path length of 10 mm was used in the UV-vis method. The MCD spectra were recorded using a Permanent Magnet PM-491 accessory and collected at a scan rate speed of 100 nm min^{-1} with a response time of 1 s, with a path length of 5 mm and in the magnetic field of +1.6 T in the N/S field direction. All spectroscopic measurements were collected in the 2.5–11 pH range, with increments of half a unit. The ligand concentration was 6×10^{-4} mol L^{-1} and the reactions were performed in a 0.3 mol L^{-1} KCl solution. Sample volumes were 2.0 mL. The pH values were obtained using a Mettler Toledo pH meter by adding small amounts of concentrated KOH and HCl solutions.

3. Results and discussion

Analysis of the potentiometric results allowed the characterization of the acid–base ability of the **BCL** ligand and the stoichiometry of the formed complexes together with their stability constants (Table 1). In the **BCL** sequence, seven functional groups are able to deprotonate: amino functions on the side-chains of five lysines and imidazole side-chains in two histidine residues (Fig. 1b). The values of $\log K$ between 10.78 and 9.26 are related to the deprotonation of the side chains of all lysine residues whilst the next two $\log K$ = 6.52 and = 5.67 are characteristic of the deprotonation of the imidazole rings on histidine side chains.

The investigated **BCL**, in contrast to the previously studied **BCS**, has two potentially independent coordinating domains due to the presence of two –KKH– motifs (Fig. 1). Owing to this fact, three systems with nL : nCu(II) molar ratios of 2 : 1, 1 : 1, and 1 : 2 were investigated and for simplicity named **A**, **B**, and **C**, respectively, c(-c(CFWKTC)-PKKHPKKHP).

In all systems, between pH 2.5 and 11, four mononuclear and seven dinuclear complexes exist (Fig. 2a, b and c). The metal binding starts with the formation of CuH_6L species (Table 1 and Fig. 2), which achieves the highest concentration around pH 4.75. Due to the low percentage of Cu(II) ions bound in this complex and the presence of other Cu(II) forms, obtainment of the spectroscopic parameters for CuH_6L was not possible. Nevertheless, the value of the corrected $\log \beta^*_{CuH_6L} = 3.81$, where $\log \beta^*_{CuH_6L} = \log \beta_{CuH_6L} - \log \beta_{H_6L}$, strongly supports the binding of one imidazole donor to the metal ion.[34] The use of the corrected stability constant makes it possible to compare these values of complexes with the same coordination mode for different peptides, regardless of what other groups are still protonated in the ligand molecule under the given conditions.

With an increase in pH, the next mononuclear CuH_5L species appears in the system. The stepwise constant for proton dissociation from CuH_6L is equal to $\log K$ = 4.65 (Table 1). Under these conditions, two hydrogen atoms are deprotonated from the ligand molecule. It can be assumed that a further deprotonating group is the imidazole of the second histidyl residue, where the metal ion may be bound. Therefore, it can be concluded that a complex with a $\{2N_{Im}\}$ coordination mode is formed here.

The values of the corrected stability constants, calculated for the complexes with only imidazole donors involved in metal ion binding, $\log \beta^*_{CuH_6L} = \log \beta_{CuH_6L} - \log \beta_{H_6L} = 3.81$ and $\log \beta^*_{CuH_5L} = \log \beta_{CuH_5L} - \log \beta_{H_5L} = 5.68$, are typical of the {1Im} and {2Im} complexes of mono-cyclopeptides,[4] but, despite the bi-cyclic structure, significantly lower than the constants calculated for the **BCS** peptide (equal to 6.24 and 8.59 for {1Im} and {2Im} complexes, respectively).[25]

Then, the CuH_4L complex is formed. The subsequent stability constant for the formation of the discussed complex is $\log K$ = 6.69 and is possibly assigned to the involvement of the first amide donor in the coordination sphere in Cu(II).[34] This species achieves the highest concentration at pH 7.4 (in **A**), pH

 This journal is © The Royal Society of Chemistry 2022

Table 1 Potentiometric data for the Cu(II)/BCL system in molar ratios of 1 : 2, 1 : 1, and 2 : 1

	BCL: c(PKKHP-c(CFWKTC)-PKKH)						
	The protonation state of the ligand						
Species	HL	H_2L	H_3L	H_4L	H_5L	H_6L	H_7L
$\log \beta$	10.78 ± 0.05	21.23 ± 0.02	31.47 ± 0.04	41.33 ± 0.02	50.59 ± 0.02	57.11 ± 0.03	62.78 ± 0.02
$\log K$	10.78 (K)	10.45 (K)	10.24 (K)	9.86 (K)	9.26 (K)	6.52 (H)	5.67 (H)

Cu(II) complexes

Species	$\log \beta$	$\log K$	Species	$\log \beta$	$\log K$
CuH_6L	60.91 ± 0.03	4.64	Cu_2H_4L	52.59 ± 0.07	13.06
CuH_5L	56.27 ± 0.01	6.89	Cu_2H_2L	39.53 ± 0.02	7.29
CuH_4L	49.38 ± 0.02	8.03	Cu_2HL	32.14 ± 0.04	9.35
CuH_3L	41.35 ± 0.03	—	Cu_2L	22.79 ± 0.02	9.09
			$Cu_2H_{-1}L$	13.70 ± 0.02	20.27
			$Cu_2H_{-3}L$	−6.57 ± 0.02	21.76
			$Cu_2H_{-5}L$	−28.33 ± 0.03	–

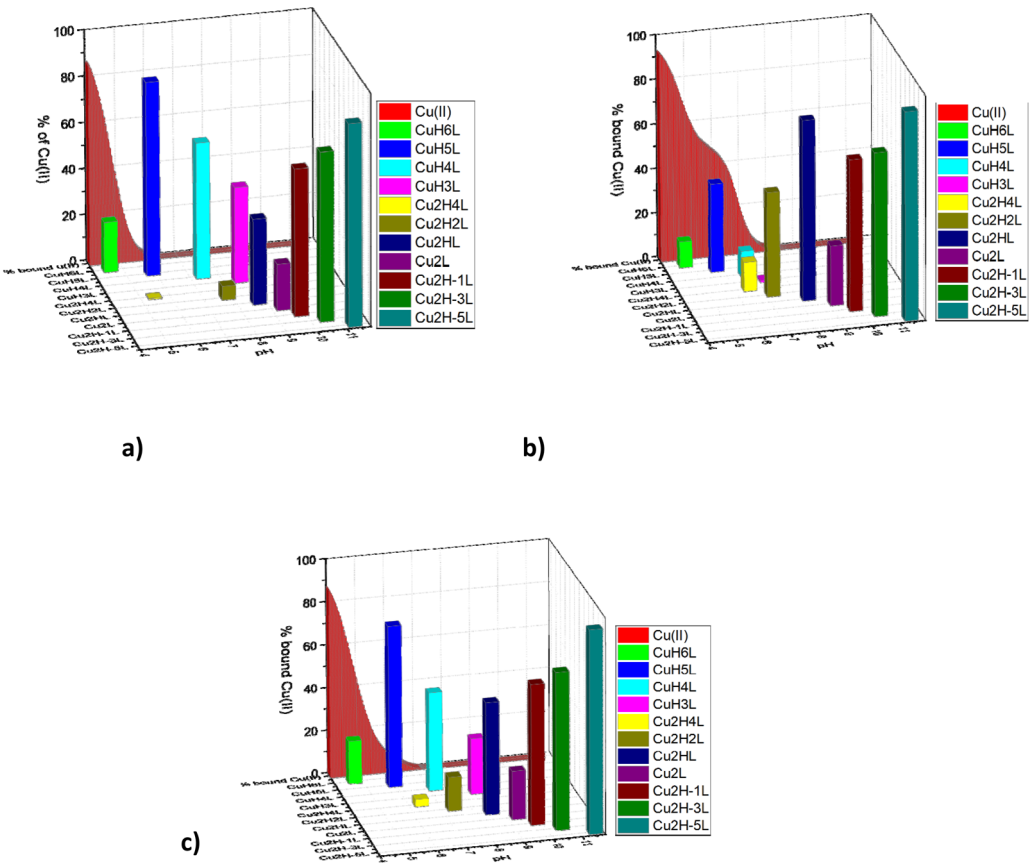

Fig. 2 The highest concentrations of the formed complexes as a function of pH in the systems with ligand to metal ion molar ratios of (**a**) 2 : 1 (**A** system), (**b**) 1 : 1 (**B** system), and (**c**) 1 : 2 (**C** system).

7.2 (in **B**), and pH 6.7 (in **C**). The percentage concentration of this species is the highest in system **A** (Fig. 2). The location of the d-d band shifts to around 579 nm in the absorption spectrum obtained for **A** (Fig. 3a) and supports the presence of three nitrogen donors in the coordination sphere of Cu(II), which may be assigned to the $\{2N_{Im}$ and $N^-_{am}\}$ binding modes.

Next, additional deprotonation and formation of CuH_3L take place, which is predominant in system **A** at pH 8 (Fig. 2a). The stepwise constant $\log K$ = 8.03 (Table 1) is related to the

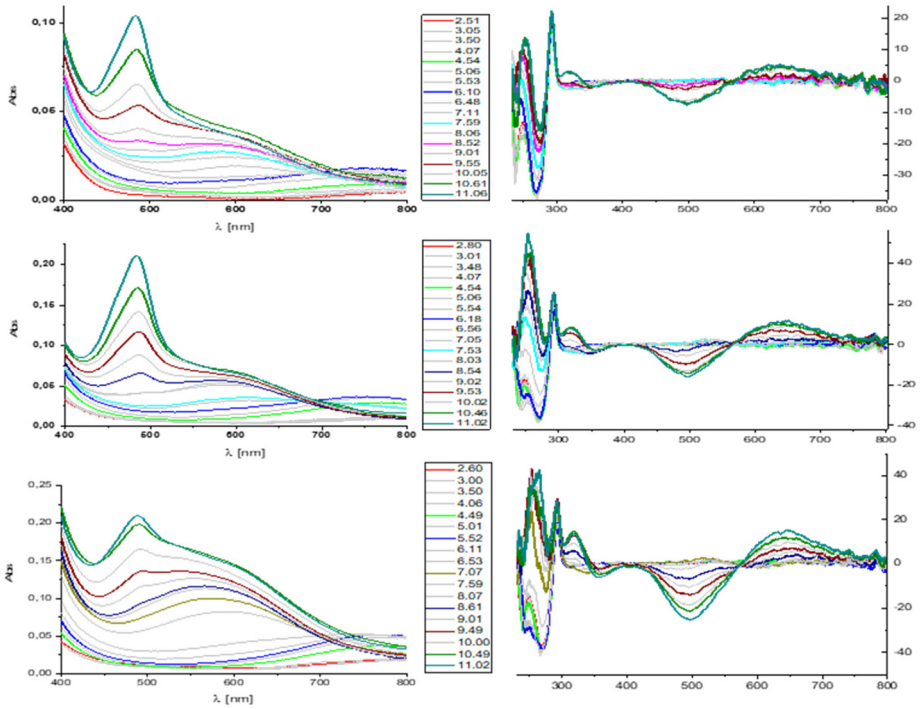

Fig. 3 The UV-vis and MCD spectra dependent on pH recorded for the **A**, **B**, and **C** systems.

proton dissociation of the second amide nitrogen. Moreover, the presence of a negative CT band at 348 nm in the MCD spectrum (Fig. 3) supports the presence of the amide donors in the coordination sphere of Cu(II). Based on these observations, we can assume that CuH_3L is characterized by the $\{2N_{Im}, 2N^-_{am}\}$ binding mode (Fig. 1).

At the same pH, di-nuclear Cu_2HL co-exists with concentrations of 30%, 45%, and 80% in the **A**, **B**, and **C** systems, respectively. Its formation forces the dissociation of two N_{Im} and four N_{am} protons. The two most likely options for the Cu(II) binding modes are a/(N_{Im}, $2N^-_{am}$)(N_{Im}, $2N^-_{am}$) and b/(N_{Im}, N^-_{am}) (N_{Im}, $3N^-_{am}$). In the absorption spectrum, obtained at pH 8, the d-d band with a λ_{max} of around 568 nm is present (Fig. 3). The theoretical λ_{max} calculated for nitrogen chromophores, located in the plane, $\{N_{Im}, N^-_{am}\}$, $\{N_{Im}, 2N^-_{am}\}$, $\{N_{Im}, 3N^-_{am}\}$ are λ_{max} = 660 nm, 564 nm and 523 nm, respectively.[33] Based on this fact, the $\{N_{Im}, 2N^-_{am}\}\{N_{Im}, 2N^-_{am}\}$ coordination set may be proposed. It is interesting that the investigated **BCL** peptide shows similar abilities to the previously studied monocyclic peptide **CMS** with the c(CHKHPHRHC) sequence.[35] At low pH, formation of the mononuclear complexes and binding to imidazole donors is preferred (Fig. 4). At higher pH values, both peptides, independent of the molar ratio, form together mono- and di-nuclear species. However, the concentration of the second species increases with an increase in the metal ion concentration.

Surprisingly, above pH 8.5, **BCL** (regardless of the metal ion concentration) forms only di-nuclear complexes in all systems with the final $Cu_2H_{-5}L$ species (Fig. 2 and 4). Due to the fact that the characterization of the binding modes for the subsequent di-nuclear complexes is difficult, detailed analysis was performed for the final $Cu_2H_{-5}L$ species. This form is predominant starting from pH 10.5 in all systems. The presence of two CT transitions, *i.e.*, one positive at around 317 nm and one negative at around 355 nm in the MCD spectra, supports the involvement of the imidazole ring and amide donors in Cu(II) binding. Its formation is related to the dissociation of all protons of the side-chains and five protons from the peptide bonds. Based on the potentiometric as well as MCD results, the $\{N_{Im}, 3N^-_{am}\}\{N_{Im}, 2N^-_{am}\}$ binding mode may be proposed.

In contrast to the recently published results for the bi-cyclopeptide **BCS**, the additional and unexpected transition at 483 nm in the UV-vis spectra appears in all systems (Fig. 3). The relationship of the intensity of the transition at 483 nm (**A**, **B**, and **C** systems) with pH, in which we observe the formation of only di-nuclear complexes, is presented in Fig. 5.

Firstly, it is clear that the intensity in system **A** is two times lower than that in **B**. This is related to the two-times lower concentration of Cu(II) (with the same ligand concentration). Secondly, in system **C**, the concentration of Cu(II) is two times higher relative to system **B**. So, one would therefore expect that the intensity should be two times higher. Nevertheless, in both systems, the intensity is almost the same. Owing to these facts it may be concluded that the appearance of this band is strictly connected with Cu(II) binding to the ligand, which specifically influences the ligand structure, and new LMCT, LLCT, or ILCT transitions are observed.

This journal is © The Royal Society of Chemistry 2022

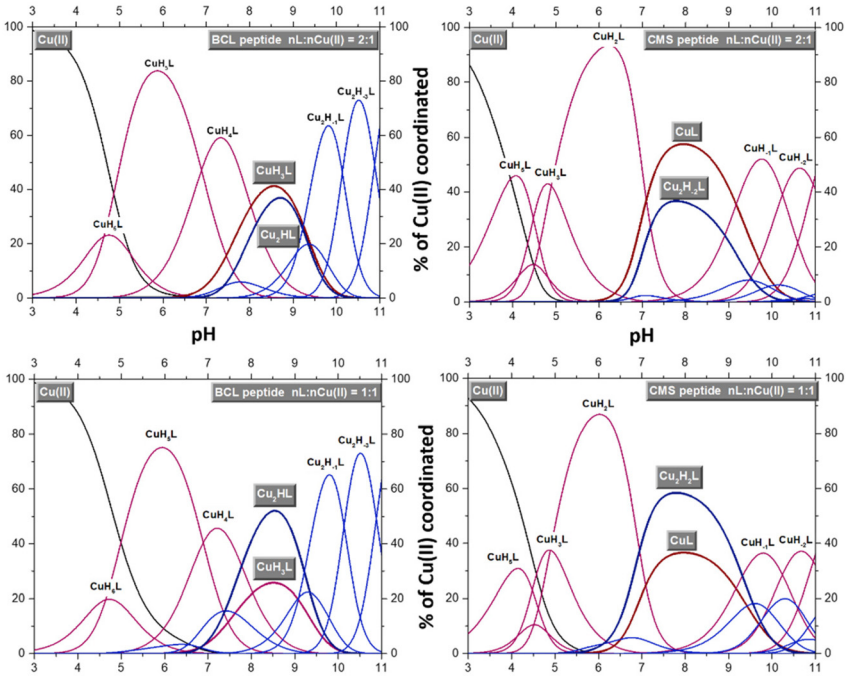

Fig. 4 Species distribution curves depending on the pH of the **BCL** and **CMS** systems. Mononuclear complexes are drawn in red and the dinuclear complexes are in blue.

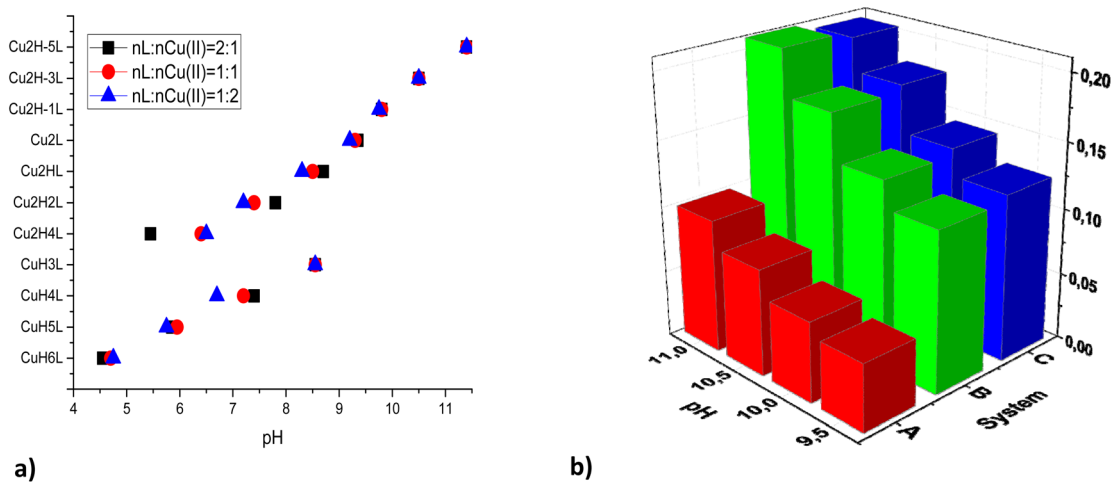

Fig. 5 (**a**) Correlation between pH and formation of the subsequent complexes in all systems; (**b**) correlation between absorbance at 483 nm, pH, and the formation of dinuclear complexes.

The investigated **BCL** ligand has in its binding motif two separated –**KKH**– sequences. The corrected stabilities for the formation of the complexes with one and two imidazole donors involved in copper (II) binding are comparable with the stabilities found for the selected cyclic and linear peptides with –**XXH**– motifs and cyclic peptides with/without disulfide bridges. The presence of the second cycle in the **BCL** molecule does not influence significantly the involvement of the first and the second amide donors also.

A significant difference is observed in the stability constants of the dinuclear $Cu_2H_{-5}L$ complex which is the lowest in the case of **BCL**. The size of the peptide cycle of **BCL** is comparable to that of the cyclic peptide presented in Table 2. This difference can be caused by the presence of the second cycle in the **BCL** molecule. The presence of two His moieties, in contrast to the c(G**NWH**PGHKHP), c(-CHKHPHRHC-) or c(HKHPHKHP), can be the other reason for the low stability of $Cu_2H_{-5}L$. However, based on the presented results, it is difficult to clearly identify the cause of the difference.

Table 2 The comparison of the corrected stability constants of one and two imidazole complexes, stepwise constants for the involvement of the first and second amide donors, and the stability constants of the $Cu_2H_{-5}L$ complexes between **BCL** and the cyclic/linear peptides with the **−XXH−** motif and 4-His-cyclic peptides with/without disulfide bridges

Mononuclear complexes

Ligand	$\log \beta^*_{n\times Im}$ $1 \times N_{Im}$	$2 \times N_{Im}$	pK N_1^-	N_2^-
BCL	3.81	5.68	6.89	8.03
c(GH**GGH**G)[36]	3.63	5.45	6.85	6.60
c(GNWHPGHKHP)[37]	—	6.03	7.63	8.02

Dinuclear complex $Cu_2H_{-5}L$

Ligand	$\log \beta_{Cu2H-5L}$
BCL	−28.33
c(G**NWH**PGHKHP)[37]	−20.37
c(-**CHKHPHRHC**-)[35]	−21.18
c(HKHPHKHP)[38]	−22.87

$\log \beta^* = \log \beta_{CuHxL} - \log \beta_{HxL}$

Conclusions

In this study, we have shown that the new synthetic bicyclic peptide **BCL**, **c(PKKHP-c(CFWKTC)-PKKH)**, which was designed for the present study, is an effective donor of copper (II) ions. In all the analyzed systems it forms both mono- and dinuclear complexes. Interestingly, above pH 8.5, we observed only complexes with two metal ions, even with an excess of the ligand system. As for the previously described bicyclic ligand **BCS**, **c(-c(CFWKTC)-PHKKHP)**, imidazole complexes are formed in the initial pH range in the analyzed metal to ligand ratios. However, those are not as thermodynamically stable as in the case of the **BCS** system. The UV-vis spectra showed the occurrence of an unexpected transition at 483 nm in all systems, which is strictly related to some sterical changes of the ligand caused by Cu(II) binding.

Author contributions

Conceptualization, J.B.; methodology, A.M., A.M.P., and J.B.; software, A.M. and J.B.; formal analysis, A.M. and J.B.; investigation, A.M., L.P., A.M.P. and J.B.; data curation, A.M., A.M.P. and J.B.; writing the original draft, A.M. and J.B.; writing the review and editing, A.M., A.M.P. and J.B.; supervision, J.B.; project administration, J.B.; funding acquisition, J.B. and A.M. P. All authors have read and agreed to the published version of the manuscript.

Conflicts of interest

There are no conflicts to declare.

Acknowledgements

This research was funded by the Wroclaw Medical University, Poland (grant number SUBZ.DO80.22.024). L. P. gratefully acknowledges MUR and EU-FSE for the financial support of the PhD fellowship PON Research and Innovation 2014–2020 (D.M 1061/2021) XXXVII Cycle in Chemical Sciences: "Greening peptide chemistry, a necessary step to the future". A. M. P. gratefully acknowledges Regione Toscana PAR-FAS (2007–2013) for supporting the Laboratory Molecular Diagnostics & Life Sciences (MoD&LS) in the context of the Centre of Competences RISE.

References

1 S. Ahangarzadeh, M. M. Kanafi, S. Hosseinzadeh, A. Mokhtarzadeh, M. Barati, J. Ranjbari and L. Tayebi, *Drug Discovery Today*, 2019, **24**, 1311–1319.
2 C. A. Rhodes and D. Pei, *Chem. – Eur. J.*, 2017, **23**, 12690–12703.
3 S. Matsunaga, N. Fusetani, K. Hashimoto and M. Walchli, *J. Am. Chem. Soc.*, 1989, **111**, 2582–2588.
4 A. M. Lengsfeld, I. Löw, T. Wieland, P. Dancker and W. Hasselbach, *Proc. Natl. Acad. Sci. U. S. A.*, 1974, **71**, 2803–2807.
5 H. Morita, K. Shimbo, H. Shigemori and J. Kobayashi, *Bioorg. Med. Chem. Lett.*, 2000, **10**, 469–471.
6 S. A. Stickel, N. P. Gomes, B. Frederick, D. Raben and T. T. Su, *Radiat. Res.*, 2015, **184**, 392–403.
7 H. Ueda, T. Manda, S. Matsumoto, S. Mukumoto, F. Nishigaki, I. Kawamura and K. Shimomura, *J. Antibiot.*, 1994, **47**, 315–323.
8 M. Fani, A. Mueller, M.-L. Tamma, G. Nicolas, H. R. Rink, R. Cescato, J. C. Reubi and H. R. Maecke, *J. Nucl. Med.*, 2010, **51**, 1771–1779.
9 M. Fani, H. R. Maecke and S. M. Okarvi, *Theranostics*, 2012, **2**, 481–501.
10 M. Fani, A. Mueller, M. L. Tamma, G. Nicolas, H. R. Rink, R. Cescato, J. C. Reubi and H. R. Maecke, *J. Nucl. Med.*, 2010, **51**, 1771–1779.
11 M. J. Stevenson, K. S. Uyeda, N. H. O. Harder and M. C. Heffern, *Metallomics*, 2019, **11**, 85–110.
12 S. A. Lambert, A. Jolma, L. F. Campitelli, P. K. Das, Y. Yin, M. Albu, X. Chen, J. Taipale, T. R. Hughes and M. T. Weirauch, *Cell*, 2018, **172**, 650–665.
13 C. W. Liew, A. Assmann, A. T. Templin, J. C. Raum, K. L. Lipson, S. Rajan, G. Qiang, J. Hu, D. Kawamori, I. Lindberg, L. H. Philipson, N. Sonenberg, A. B. Goldfine, D. A. Stoffers, R. G. Mirmira, F. Urano and R. N. Kulkarni, *Proc. Natl. Acad. Sci. U. S. A.*, DOI: **10.1073/pnas.1323066111**.
14 A. Mizutani, H. Inoko and M. Tanaka, *Mol. Cells*, 2016, **39**, 756–761.
15 M. R. Sapio and L. D. Fricker, *Proteomics: Clin. Appl.*, 2014, **8**, 327–337.
16 E. C. Lee, E. Ha, S. Singh, L. Legesse, S. Ahmad, E. Karnaukhova, R. P. Donaldson and A. M. Jeremic, *Phys. Chem. Chem. Phys.*, 2013, **15**, 12558–12571.
17 A. F. Pearlmutter and M. S. Soloff, *J. Biol. Chem.*, 1979, **254**, 3899–3906.

 This journal is © The Royal Society of Chemistry 2022

18 T. Kleszczewski, B. Modzelewska, W. Bal, M. Sipowicz and A. Kostrzewska, *Contraception*, 2003, **67**, 477–483.
19 D. Liu, A. B. Seuthe, O. T. Ehrler, X. Zhang, T. Wyttenbach, J. F. Hsu and M. T. Bowers, *J. Am. Chem. Soc.*, 2005, **127**, 2024–2025.
20 X. Xu, W. Yu, Z. Huang and Z. Lin, *J. Phys. Chem. B*, 2010, **114**, 1417–1423.
21 T. Wyttenbach, D. Liu and M. T. Bowers, *J. Am. Chem. Soc.*, 2008, **130**, 5993–6000.
22 A. Marciniak, Z. Czyznikowska, M. Cebrat, A. Kotynia and J. Brasuń, *Inorg. Chim. Acta*, 2014, **416**, 57–62.
23 A. Marciniak, A. Kotynia, M. Cebrat and J. Brasuń, *Int. J. Pept. Res. Ther.*, 2020, **26**, 969–977.
24 A. Marciniak, M. Cebrat and J. Brasuń, *Int. J. Pept. Res. Ther.*, 2017, **23**, 135–143.
25 A. Marciniak, W. Witak, G. Sabatino, A. M. Papini and J. Brasuń, *Int. J. Mol. Sci.*, 2020, **21**, 1–13.
26 A. Marciniak, M. Cebrat, Z. Czyznikowska and J. Brasuń, *J. Inorg. Biochem.*, 2012, **117**, 10–17.
27 A. Marciniak, W. Witak, A. Pieniężna and J. Brasun, *Chem. Biodiversity*, 2020, cbdv.202000307.
28 F. Nuti, E. Peroni, F. Real-Fernández, M. A. Bonache, A. Le Chevalier-Isaad, M. Chelli, N. Lubin-Germain, J. Uziel, P. Rovero, F. Lolli and A. M. Papini, *Biopolymers*, 2010, **94**, 791–799.
29 F. Rizzolo, C. Testa, D. Lambardi, M. Chorev, M. Chelli, P. Rovero and A. M. Papini, *J. Pept. Sci.*, 2011, **17**, 708–714.
30 G. Sabatino, M. Chelli, S. Mazzucco, M. Ginanneschi and A. M. Papini, *Tetrahedron Lett.*, 1999, **40**, 809–812.
31 H. M. Irving, M. G. Miles and L. D. Pettit, *Anal. Chim. Acta*, 1967, **38**, 475–488.
32 P. Gans, A. Sabatini and A. Vacca, *J. Chem. Soc., Dalton Trans.*, 1985, 1195–1200.
33 P. Gans, A. Sabatini and A. Vacca, *Talanta*, 1996, **43**, 1739–1753.
34 A. Kotynia, J. S. Pap and J. Brasun, *Inorg. Chim. Acta*, 2018, **472**, 3–11.
35 A. Pieniężna, W. Witak, A. Szymańska and J. Brasuń, *Int. J. Mol. Sci.*, 2021, **22**, 6458, DOI: **10.3390/ijms22126458**.
36 R. P. Bonomo, G. Impellizeri, G. Pappalardo, R. Purrello, E. Rizzarelli and G. Tabbi, *J. Chem. Soc., Dalton Trans.*, 1998, 3851–3857.
37 A. Fragoso, R. Delgado and O. Iranzo, *Dalton Trans.*, 2013, **42**, 6182–6192.
38 A. Kotynia, S. Bielińska, W. Kamysz and J. Brasuń, *Dalton Trans.*, 2012, **41**, 12114–12120.

This journal is © The Royal Society of Chemistry 2022